

PAPER REF: 6562

## **AN ALGORITHM FOR DAMAGE DETECTION AND LOCALIZATION USING OUTPUT-ONLY RESPONSE FOR CIVIL ENGINEERING STRUCTURES SUBJECTED TO SEISMIC EXCITATIONS**

**Farouk Frigui<sup>1,2(\*)</sup>, Jean-Pierre Faye<sup>1</sup>, Carmen Martin<sup>1</sup>, Olivier Dalverny<sup>1</sup>, François Peres<sup>1</sup>, Sébastien Judenherc<sup>2</sup>**

<sup>1</sup>Ecole Nationale d'Ingénieurs de Tarbes, LGP, 47 avenue d'Azereix, 65016 Tarbes, France

<sup>2</sup>STANEO, 2 rue Marcel Langer 31600 Seysses, France

(\*)Email: ffrigui@enit.fr

### **ABSTRACT**

Structure damage in civil engineering is generally caused by natural aging of materials, human activities or natural disasters. Control and monitoring of the structure's health (SHM) present a very important stake for human and material security. In this context, many methods based on structure dynamic behaviour allow detection or localization of structural damages, especially concerning structures submitted to seismic excitations. These SHM technics are usually called Vibration-Based Damage Detection Methods (VBDDM). Every method of detection and localization depends on the accuracy of the experimental identification of modal parameters using Operational Modal Analysis (OMA), as well as number of modes and sensors. So far, no method enables, in simple and quick procedure, a precise detection and localization while having the optimal conditions: minimal number of sensors, use of low order modes. In this paper, we propose a new algorithm using in the first place, Covariance-driven stochastic subspace identification method (SSI-COV) to estimate modal parameters and in the second place, some VBDDM methods to reach a good detection and localization level for robust SHM applications. In order to evaluate our approach, a finite element model of reinforced concrete building is established.

**Keywords:** SHM, vibration, OMA, Output-only analysis, damage detection and localization.

### **INTRODUCTION**

Control and monitoring of a structure in civil engineering, in order to guarantee its good functioning, are based on its vibrational behaviour's analysis. These technics consist in following the evolution of dynamic features such as: Eigen frequencies, mode shapes, flexibility (Ndambi, 2002). In practice, these technics help choosing actions of rehabilitation on damaged structures, leading consequently to an optimization of maintenance costs. The technics generally used are Frequency-Based Damage Detection methods (FBDD) and Mode-shapes-Based Damage Detection methods (MBDD). Previous studies showed that the FBDD methods are easy to implement experimentally, very sensitive to damage, but very difficult to interpret in cases of low variations (Yan, 2007). However, MBDD methods are more precise and allow detection and localization of damages (Kim, 2003). Precision can be improved by using an important number of sensors and high order modes, which turns out to be difficult to realise experimentally. In the work related here, we propose a global method gathering various VBDDM technics in order to obtain better precision. This global method present three levels: Modal parameter identification, detection and localization.

## COVARIANCE-DRIVEN STOCHASTIC SUBSPACE IDENTIFICATION METHOD

### 1. Theoretical background

#### 1.1. State space models

In the case of a time-invariant linear dynamic model, the behaviour of the structure is described by the differential system (Goursat, 2001):

$$\begin{cases} M\ddot{Z}(t) + C\dot{Z}(t) + KZ(t) = v(t) \\ Y(t) = C_a\ddot{Z}(t) + C_v\dot{Z}(t) + C_dZ(t) \end{cases} \quad (1)$$

Where  $Z(t)$ ,  $\dot{Z}(t)$  and  $\ddot{Z}(t)$  are respectively: the displacement, velocity, and acceleration vectors of the considered degrees of freedom.  $M$ ,  $C$  and  $K$  are respectively the mass, damping and stiffness matrices. The excitation  $v(t)$  is considered as zero-mean white noise.  $Y(t)$  is the output vector which is a combination of the accelerations, velocities and displacements vectors.  $C_a$ ,  $C_v$  and  $C_d$  are the selection matrices (Reynders, 2007).

The Eigen frequencies  $\chi$  and the Eigenvectors  $\{\psi\}$  are deduced from the equations below:

$$\begin{cases} \det(M\chi^2 + C\chi + K) = 0 \\ (M\chi^2 + C\chi + K) \psi_\chi = 0 \end{cases} \quad (2)$$

By a change of variable:  $X(t) = \begin{pmatrix} Z(t) \\ \dot{Z}(t) \end{pmatrix}$ , a state vector, equation (1) can be rewritten as:

$$\begin{cases} \dot{X}(t) = A_c X(t) + B_c v(t) \\ Y(t) = C_c X(t) + D_c v(t) \end{cases} \quad (3)$$

Where  $B_c = \begin{bmatrix} 0 \\ M^{-1} \end{bmatrix}$  and  $D_c = C_a M^{-1}$  are respectively the process noise and the measurement noise matrices;  $C_c = [C_d - C_a M^{-1} K \quad C_v - C_a M^{-1} K]$  is the observation matrix and  $A_c = \begin{bmatrix} 0 & I \\ -M^{-1} K & -M^{-1} C \end{bmatrix}$  is the transition matrix.

Equation (3) is also called the state-space model in continuous time.

By discretizing in time, the state space model can be written as:

$$\begin{cases} x_{(k+1)} = Ax_{(k)} + w_{(k)} \\ y_{(k)} = Cx_{(k)} + q_{(k)} \end{cases} \quad (4)$$

Where  $x_{(k+1)}$  is the  $(2n \times 1)$  state vector at the time instant  $(k+1)\Delta T$ ,  $\Delta T$  is the sampling period.;  $y_{(k)}$  is the  $(l \times 1)$  output vector at the time instant  $k\Delta T$ .  $w \in R^{2n \times 1}$  and  $q \in R^{l \times 1}$  are respectively the process and the measurement noises in discrete-time and are assumed to be a zero-mean samples ( $E(w_{(k)} x_{(k)}^t) = 0$  and  $E(q_{(k)} x_{(k)}^t) = 0$ );  $A = e^{A_c \Delta T}$  is the transition matrix in discrete-time and  $C = \int_{k\Delta T}^{k\Delta T + \Delta T} e^{A_c(k\Delta T + \Delta T - \tau)} d\tau B_c$  is the observation matrix in discrete-time.

The purpose of the SSI-COV's algorithm is to identify the transition matrix  $A$  which contains all the modal information (Zhang, 2012; Peeters, 2000).

## 1.2. Covariance matrices

Before presenting the approach of the SSI-COV's algorithm, we introduce the notion of covariance in order to establish a relation between the output vector  $y(t)$  and the state vector  $x(t)$ . In fact, covariance allows cancelling the white noise and bringing up the transition matrix  $A$  through mathematical means.

The covariance matrices of the white noises  $(w_{(k)}, q_{(k)})$  and the state vector  $x_{(k+1)}$  is zero since  $w_{(k)}$  and  $q_{(k)}$  are zero-mean samples.

$$\begin{cases} E(w_{(k)}x_{(k)}^t) = 0 \\ E(q_{(k)}x_{(k)}^t) = 0 \end{cases} \quad (5)$$

The expression of the state vector  $x_{(k+i)}$  is derived from the equation  $x_{(k+1)} = Ax_{(k)} + w_{(k)}$  by recurrence as follows:

$$\begin{aligned} x_{(k+i)} &= Ax_{(k+i-1)} + w_{(k+i-1)} \\ &= A(Ax_{(k+i-2)} + w_{(k+i-1)}) + w_{(k+i-1)} \\ &\dots \\ &= A^i x_{(k)} + A^{i-1} w_{(k)} + A^{i-2} w_{(k+1)} + \dots + Aw_{(k+i-2)} + w_{(k+i-1)} \end{aligned} \quad (6)$$

The covariance matrix of the state vector  $x_{(k)}$  can be written as:

$$\Sigma_{xx} = E(x_{(k)}x_{(k)}^t) \quad (7)$$

The covariance matrix of the state vector  $x_{(k+1)}$  can be written as:

$$\begin{aligned} \Sigma_{xx1} &= E(x_{(k+1)}x_{(k+1)}^t) \\ &= E((Ax_{(k)} + w_{(k)})(A^t x_{(k)}^t + w_{(k)}^t)) \\ &= E(Ax_{(k)}A^t x_{(k)}^t) + E(Ax_{(k)}w_{(k)}^t) + E(w_{(k)}A^t x_{(k)}^t) + E(w_{(k)}w_{(k)}^t) \\ &= AE(x_{(k)}x_{(k)}^t)A^t + AE(x_{(k)}w_{(k)}^t) + A^t E(w_{(k)}x_{(k)}^t) + E(w_{(k)}w_{(k)}^t) \\ &= AE(x_{(k)}x_{(k)}^t)A^t + AE(x_{(k)}w_{(k)}^t) + A^t E(w_{(k)}x_{(k)}^t) + E(w_{(k)}w_{(k)}^t) \\ &= A\Sigma_{xx}A^t + Q_e \end{aligned} \quad (8)$$

The covariance matrix of the state vector  $x_{(k+1)}$  and the output vector  $y_{(k)}$  can be written as:

$$\begin{aligned} G &= E(x_{(k+1)}y_{(k)}^t) \\ &= E((Ax_{(k)} + w_{(k)})(C^t x_{(k)}^t + q_{(k)}^t)) \\ &= E(Ax_{(k)}C^t x_{(k)}^t) + E(Ax_{(k)}q_{(k)}^t) + E(w_{(k)}C^t x_{(k)}^t) + E(w_{(k)}q_{(k)}^t) \\ &= AE(x_{(k)}x_{(k)}^t)C^t + E(Ax_{(k)}q_{(k)}^t) + E(w_{(k)}C^t x_{(k)}^t) + E(w_{(k)}q_{(k)}^t) \\ &= A\Sigma_{xx}C^t + E(Ax_{(k)}q_{(k)}^t) + E(w_{(k)}C^t x_{(k)}^t) + E(w_{(k)}q_{(k)}^t) \\ &= A\Sigma_{xx}C^t + E(w_{(k)}q_{(k)}^t) \\ &= A\Sigma_{xx}C^t + S \end{aligned} \quad (9)$$

The covariance matrix of the output vector  $y_{(k)}$  can be written as:

$$\begin{aligned}
 \Lambda_0 &= E(y_{(k)}y_{(k)}^t) \\
 &= E((Cx_{(k)} + q_{(k)})(C^t x_{(k)}^t + q_{(k)}^t)) \\
 &= E(Cx_{(k)}C^t x_{(k)}^t) + E(Cx_{(k)}q_{(k)}^t) + E(q_{(k)}C^t x_{(k)}^t) + E(q_{(k)}q_{(k)}^t) \\
 &= CE(x_{(k)}x_{(k)}^t)C^t + R \\
 &= C\Sigma_{xx}C^t + R
 \end{aligned} \tag{10}$$

From equations (6) and (9) we can assess the covariance matrix of the output vectors  $y_{(k+i)}$  and  $y_{(k)}$ :

$$\begin{aligned}
 \Lambda_i &= E(y_{(k+i)}y_{(k)}^t) \\
 &= E((Cx_{(k+i)} + q_{(k+i)})(C^t x_{(k)}^t + q_{(k)}^t)) \\
 &= E((C(A^i x_{(k)} + A^{i-1}w_{(k)} + A^{i-2}w_{(k+1)} + \dots + Aw_{(k+i-2)} + w_{(k+i-1)}) + q_{(k+i)})(C^t x_{(k)}^t + q_{(k)}^t)) \\
 &= E((CA^i x_{(k)} + CA^{i-1}w_{(k)} + CA^{i-2}w_{(k+1)} + \dots + CAw_{(k+i-2)} + Cw_{(k+i-1)} + q_{(k+i)})(C^t x_{(k)}^t + q_{(k)}^t)) \\
 &= E((CA^i x_{(k)}C^t x_{(k)}^t + CA^{i-1}w_{(k)}C^t x_{(k)}^t + CA^{i-2}w_{(k+1)}C^t x_{(k)}^t + \dots + CAw_{(k+i-2)}C^t x_{(k)}^t + Cw_{(k+i-1)}C^t x_{(k)}^t + q_{(k+i)}C^t x_{(k)}^t + (CA^i x_{(k)}q_{(k)}^t + CA^{i-1}w_{(k)}q_{(k)}^t + CA^{i-2}w_{(k+1)}q_{(k)}^t + \dots + CAw_{(k+i-2)}q_{(k)}^t + Cw_{(k+i-1)}q_{(k)}^t + q_{(k+i)}q_{(k)}^t)) \\
 &= E((CA^i x_{(k)}C^t x_{(k)}^t) + (CA^{i-1}w_{(k)}q_{(k)}^t)) \\
 &= CA^i E(x_{(k)}x_{(k)}^t)C^t + CA^{i-1}E(w_{(k)}q_{(k)}^t) \\
 &= CA^i \Sigma_{xx} C^t + CA^{i-1}S \\
 &= CA^{i-1}(A\Sigma_{xx}C^t + S) \\
 &= CA^{i-1}G
 \end{aligned} \tag{11}$$

From equation (11), one can see the relation between the state vector  $x_{(k)}$  and the output vector  $y_{(k)}$  as well as the appearance of the transition matrix  $A$  (Xie, 2016).

## 2. Covariance-Driven Stochastic Subspace Identification Algorithm

The four steps of SSI-COV's algorithm are summarized in Fig.1. Details are presented in the next paragraphs.

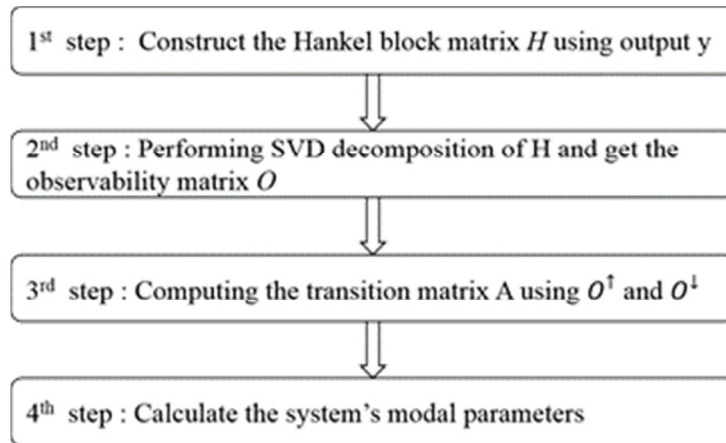


Fig. 1 - Flowchart of the SSI-COV's algorithm

### 2.1. Hankel block matrix:

The first step of SSI-COV's algorithm is to gather the covariance matrices of the output into the block Hankel matrix  $H$  ( $(p+1) \times q$ ) as follows (Döhler, 2013):

$$\begin{aligned}
 H &= \begin{bmatrix} \Lambda_1 & \Lambda_2 & \dots & \Lambda_q \\ \Lambda_2 & \vdots & \vdots & \Lambda_{q+1} \\ \vdots & \vdots & \vdots & \vdots \\ \Lambda_{p+1} & \Lambda_{p+2} & \dots & \Lambda_{p+q} \end{bmatrix} = \begin{bmatrix} CA^0G & CA^1G & \dots & CA^{q-1}G \\ CA^1G & \vdots & \vdots & CA^qG \\ \vdots & \vdots & \vdots & \vdots \\ CA^pG & CA^{p+1}G & \dots & CA^{p+q-1}G \end{bmatrix} \\
 &= \begin{pmatrix} C \\ CA \\ CA^2 \\ \vdots \\ CA^p \end{pmatrix} (G \quad GA \quad GA^2 \quad \dots \quad GA^{q-1}) = O * K
 \end{aligned} \tag{12}$$

Where  $O$  is the observability matrix and  $K$  is the controllability matrix (Van Overschee, 1996; Mevel, 2004).

One of the widely-used methods, in order to compute the transition matrix  $A$ , is based on the observability matrix  $O$ .

### 2.2. Observability Matrix:

The observability matrix is computed, in the second step, from the decomposition of the block Hankel matrix  $H$  into three matrices  $U$ ,  $S$  and  $V$  using the single value decomposition (SVD):

$$\begin{aligned}
 H &= USV^t = [U_1 \quad U_2] \begin{bmatrix} S_1 & 0 \\ 0 & S_2 \cong 0 \end{bmatrix} [V_1^t \quad V_2^t] = U_1 S_1 V_1^t \\
 H &= U_1 S_1^{0.5} S_1^{0.5} V_1^t
 \end{aligned} \tag{13}$$

Comparing equation (12) with equation (13) one obtains:

$$O = \begin{pmatrix} C \\ CA \\ CA^2 \\ \vdots \\ CA^p \end{pmatrix} = U_1 S_1^{0.5} \tag{14}$$

### 2.3. Transition Matrix:

In the third step, from the observability matrix  $O$ ,  $O^\uparrow$  is obtained by removing the last block row and  $O^\downarrow$  is obtained by removing the first block row (Wu 2016):

$$O^\uparrow = \begin{pmatrix} C \\ CA \\ CA^2 \\ \vdots \\ CA^{p-1} \end{pmatrix} \tag{15}$$

$$O^\downarrow = \begin{pmatrix} CA \\ CA^2 \\ \vdots \\ \vdots \\ CA^p \end{pmatrix} = A \begin{pmatrix} C \\ CA \\ CA^2 \\ \vdots \\ CA^{p-1} \end{pmatrix} = AO^\uparrow \quad (16)$$

From equation (16) one obtains the transition matrix  $A$ :

$$A = O^\uparrow O^\downarrow\# \quad (17)$$

## 2.4. Eigen frequencies identification:

In the final step, Eigen frequencies are then computed from Eigenvalues ( $\lambda_i$ ) of the transition matrix  $A$  as follows:

$$\lambda_i = e^{\lambda_{ci}\Delta T} \quad (18)$$

$$\lambda_{ci} = \frac{\ln(\lambda_i)}{\Delta T} \quad (19)$$

$$f_i = w_i/2\pi = \sqrt{Re(\lambda_{ci})^2 + Im(\lambda_{ci})^2}/2\pi \quad (20)$$

Where  $\lambda_{ci}$  are the Eigenvalues of the transition matrix  $A_c$  and  $w_i$  is the  $i^{\text{th}}$  angular frequency.

## VIBRATION-BASED DAMAGE DETECTION AND LOCALIZATION METHODS

The change in the physical properties of a structure (Young's modulus, stiffness...etc.) systematically induces a change in its dynamic characteristics (Eigen frequencies, mode shapes, damping...etc.). Indeed, when the structure is damaged, the stiffness  $K$  decreases and the damping factor  $\zeta$  increases with reduction of the Eigen frequencies and modification of the mode shapes. Thus, the monitoring of the dynamic characteristics represents an accurate method of evaluation of the structure health.

The problem lies in establishing a correct correlation between the variation of the dynamic characteristics, the occurrence of the damage, its location, size, severity and impact on the performance of the structure.

### 1. Vibration-based damage detection methods

#### 1.1. Eigen frequencies changes

The presence of damage in the structure induces a change in its behaviour. Since, the Eigen frequencies reflect the overall behaviour of the structure, the monitoring of the frequencies is a sensitive damage indicator (Yan 2007). This method provides an inexpensive mean for Structural Health Monitoring. In fact, once the Eigen frequencies are identified, the implementation of this method is easy and carried out as follows (Salawu, 1997; Lee 2000):

$$\Delta f = f_{j-i} - f_{j-f} \quad (21)$$

Where  $f_{j-i}$  is the  $j^{\text{th}}$  Eigen frequency of the initial state (before damage) and  $f_{j-f}$  is the  $j^{\text{th}}$  Eigen frequency of the final state (after damage).

## 1.2. Modal assurance criterion

The modal assurance criterion (MAC) is a comparison criterion based on mode shapes (Pastor, 2012). The criterion returns a matrix with values ranging between 0 and 1. Any value equal to 1 corresponds to a complete correlation between two measurement sets. Any value between 0 and 1 corresponds to an incomplete correlation (Ndambi, 2002). The criterion is computed as follows:

$$MAC_{jk} = \frac{[\sum_{i=1}^n [\Psi_A]_i^j [\Psi_B]_i^k]^2}{\sum_{i=1}^n ([\Psi_A]_i^j)^2 \sum_{i=1}^n ([\Psi_B]_i^k)^2} \quad (22)$$

Where  $\Psi_A$  and  $\Psi_B$  are respectively the undamaged and the damaged sets of mode shapes.

The aim of this criterion is to compare a set of initial mode shapes with a set of final mode shapes at the same mode  $j$  ( $MAC_{jj}$ ). The derivation of the  $MAC_{jj}$ 's values from 1 could be interpreted as a damage indication (Abozeid, 2006).

## 2. Vibration-based damage localization methods

### 2.1. Mode shape curvature changes and curvature damage factor

The mode shape curvature allows not only to detect but also to locate structural damages. This method is very sensitive, at lower modes, to small disturbances caused by damages (Rucevskis, 2010; Pandey, 1991).

From the mode shape displacements, and using the central difference approximation, mode shape curvatures are computed as follows:

$$v''_{i,j} = (v_{i+1,j} - 2v_{i,j} + v_{i-1,j})/h^2 \quad (23)$$

$$\Delta v''_{i,j} = |v''_{i,j}{}^u - v''_{i,j}{}^d| \quad (24)$$

Where  $v_{i,j}$  is the displacement corresponding to the  $i^{th}$  node and  $j^{th}$  mode;  $h$  is the distance between two consecutive measurement nodes.  $v''_{i,j}$  represent the mode shape curvature at the  $i^{th}$  node and  $j^{th}$  mode.  $u$  and  $d$  are indexes associated to the undamaged and damaged structures.

In order to reach global information concerning the damage, one can use the curvature damage factor (CDF) which is derived from the method of mode shape curvature change (Wahab, 1999). It consists in averaging the variations of the mode shape curvature at a given node with respect to the number of considered modes. CDF seems to be an accurate damage detector especially when several damages are presented in the structure (Foti, 2013; Tripathy, 2004). This method is computed as follows:

$$CDF = \frac{\sum_{n=1}^N |v''_{i,j}{}^u - v''_{i,j}{}^d|}{N} \quad (25)$$

Where  $N$  is the total number of modes.

The accuracy of detection and localization depends on the number of measurement nodes. In other words, the more complete the description of the mode shape, the more accurate the localization of the damaged area is (Abozeid, 2006; Dawari, 2013).

## 2.2. Flexibility changes

The presence of a damage in the structure induces a stiffness decrease while flexibility increase. Furthermore, the flexibility method allows detection and accurate localization of the damage. Moreover, the flexibility converges rapidly by increasing the frequency, thus a few lower mode frequencies provide a good estimation of the flexibility matrix (Ndambi, 2002). The flexibility method is computed as follows:

$$F = \sum_{i=1}^n \frac{1}{w_i^2} \varphi_i \varphi_i^t \quad (26)$$

$$\Delta F = F_i - F_f \quad (27)$$

Where  $w_i$  is the  $i^{th}$  modal frequency;  $\varphi = [\varphi_1 \ \varphi_2 \ \dots \ \varphi_n]$  is the mode shape matrix,  $F$  the flexibility matrix;  $\Delta F$  the flexibility variation matrix;  $F_i$  the initial flexibility matrix corresponding to the undamaged structure and  $F_f$  the final flexibility matrix corresponding to the damaged structure.

For every measurement node  $j$ , we define  $\bar{Y}_j$  as the maximum absolute value of the corresponding column of  $\Delta F$ :

$$\bar{Y}_j = \max_i |\Delta F_{ij}| \quad (28)$$

$\bar{Y}_j$  shows the variation of the flexibility along the measurement nodes, and thus presents a damage indicator (Pandey, 1994). This method is valid as long as the mode shapes are mass-normalized to unity ( $\varphi^t M \varphi = 1$ ).

## NUMERICAL SIMULATION

### 1. Finite element model (FEM)

The test case is a 6-storey building, shown in Fig.2. The model was conceived using shell element model and the properties of aged reinforced concrete ( $E_{(young's \ modulus)} = 12 \text{ GPa}$ ,  $\nu_{(poisson's \ ratio)} = 0.2$ , shell thickness = 0.15 m).

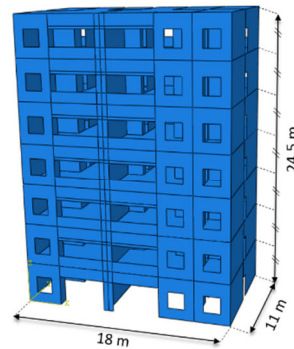


Fig. 2 - Finite element model of a 6-storey building

The seismic damage was modelled by a reduction of 80% in Young's modulus at the 4<sup>th</sup> floor as shown in Fig.3(a). It's also assumed that 4 sensors are used in order to record accelerations. The position of sensors (measurement nodes) are shown in Fig.3 (b).

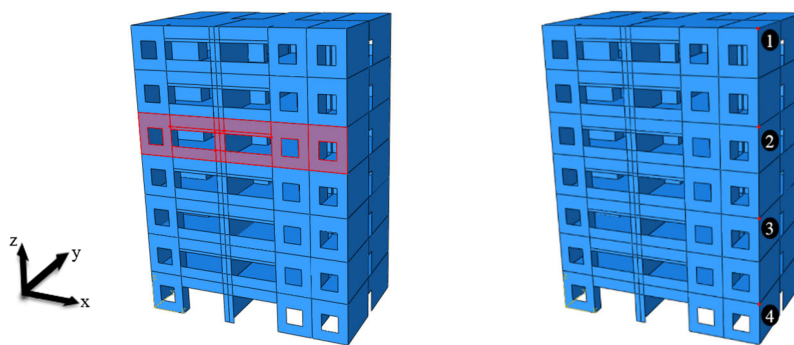


Fig. 3 - (a) Damaged building - (b) Sensors locations

The structure was excited with a zero-mean white noise excitation for 25 seconds in the  $\vec{x}$  direction. The accelerations of nodes are recorded in both directions  $\vec{x}$  and  $\vec{y}$  in order to identify the first Eigen frequencies, with the sampling period  $T_e = 0.01s$ .

The numerical procedure is presented in Fig.4. The aim of the new algorithm is to detect and locate damages following three levels:

- 1- Identification of modal parameters using the SSI-COV algorithm.
- 2- Damage detection using frequencies changes method and MAC.
- 3- Damage localization using mode shape curvature method, CDF and flexibility changes.

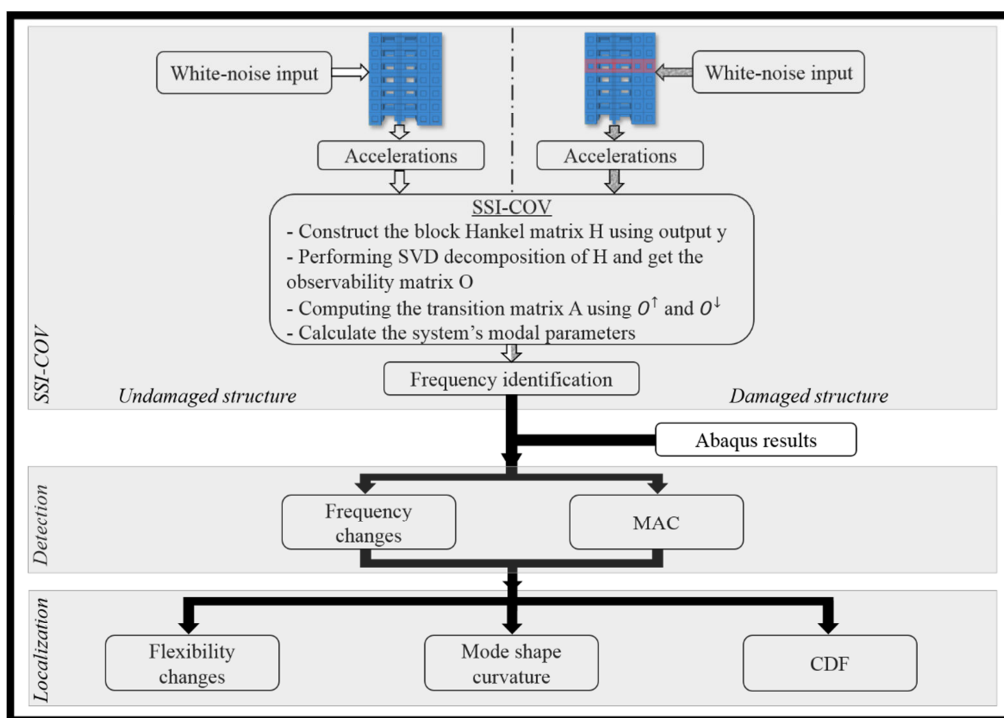


Fig. 4 - Flowchart of numerical simulation

The SSI-COV's algorithm was applied to identify the Eigen frequencies of the 6-storey building. Eigen frequencies are then used in the detection and localization levels. Frequencies changes and MAC methods are applied in the first place for their simplicity and sensitivity to damage. Once the damage is detected, one can move to the localization level.

## 2. Eigen Frequencies Identification

SSI-COV's algorithm results are compared with Abaqus results in both situations: undamaged and damaged structures. The first 5 Eigen frequencies are presented in table 1. The results show a good estimation of the Eigen frequencies using SSI-COV algorithm (the frequency's relative error are smaller than 2%).

Table 1 - Comparison of identified parameters between SSI-COV and Abaqus

Mode n°	Undamaged structure			Damaged structure		
	$F_{abaqus}$ (Hz)	$F_{SSI-cov}$ (Hz)	Error (%)	$F_{abaqus}$ (Hz)	$F_{SSI-cov}$ (Hz)	Error (%)
1	3.22	3.22	0	3.16	3.16	0
2	4.05	4.12	+1.7	4.03	4.1	+1.7
3	5.7	5.68	-0.35	5.58	5.55	-0.54
4	10.3	10.25	-0.49	10.06	10.04	-0.2
5	13.16	13.2	+0.3	12.96	13	+0.3

## 3. Damage detection

The changes in the identified frequencies showed that Eigen frequencies are very sensitive to damage. Indeed, we noticed a reduction of 1.86% in the 1<sup>st</sup> mode frequency and a reduction of 2.33% in the 4<sup>th</sup> mode frequency using Abaqus results (Fig.5(a)). We also noticed a reduction of 1.86% in the 1<sup>st</sup> mode frequency and a reduction of 2.28% in the 3<sup>rd</sup> mode frequency using SSI-COV algorithm (Fig.5(b)).

We can conclude from above that changes in Eigen frequencies (i) can be considered as a good damage indicator, (ii) are very easy to set-up but (iii) are not suitable to locate damage.

The modal assurance criterion compares the displacements of all the measurement nodes in the undamaged state with respect to their displacement in the damaged state at a given mode j (equation (21)). Thus, the use of all measurement nodes does not permit localization but only the detection of changes in mode shape due to damage.

In Fig.6, we observe a value of 0.87 (close to 1) which indicates a small change in the mode shapes, specifically in the 5<sup>th</sup> mode and therefore a probable damage.

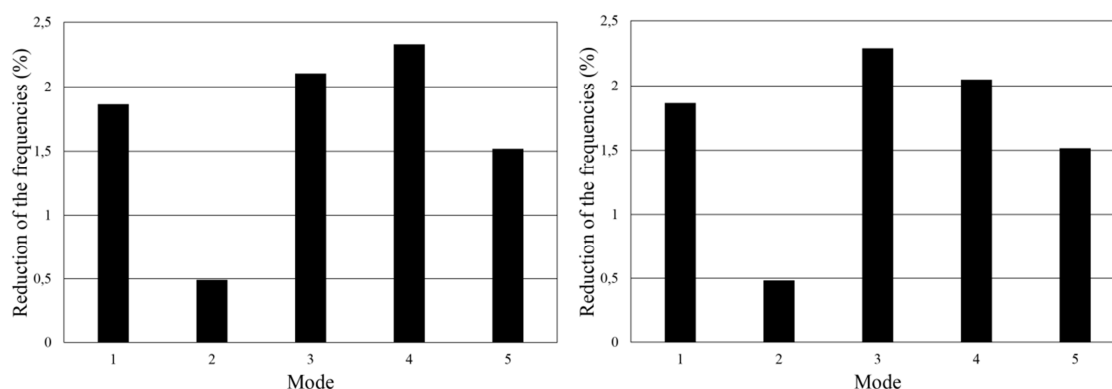


Fig. 5 - (a) Frequencies changes using Abaqus results - (b) Frequencies changes using SSI-COV algorithm

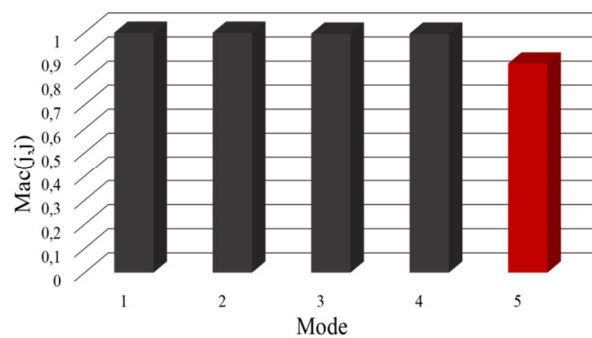


Fig. 6 - Modal assurance criterion applied to the first 5 modes

#### 4. Damage localization

By using the mode shape curvature method applied to the first mode and the CDF applied to the first 5 modes, it was found that the largest variations were located at sensors 2 and 3 which surround the damaged storey (Fig.7).

Regarding the flexibility method, the flexibility matrix is achieved using the first two modes. The damage was located between sensors 2 and 3. In fact, when the structure is damaged, its rigidity decreases while flexibility increases. Starting from the bottom to the top (from sensor 4 to sensor 1), one can notice a sudden increase in the flexibility located between sensors 3 and 2. This zone has probably undergone a structural weakening, and therefore a decrease of its stiffness (Fig.8).

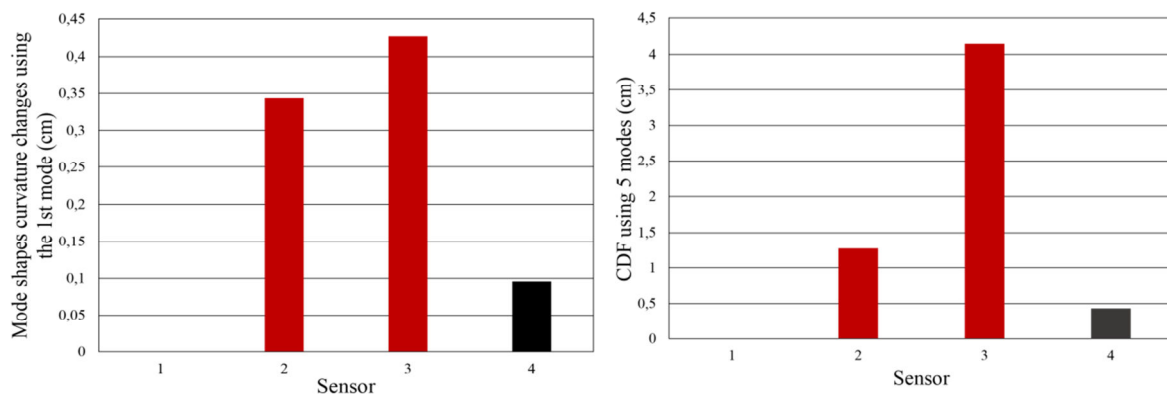


Fig. 7 - (a) Mode shapes curvature changes using the 1<sup>st</sup> mode - (b) Curvature damage factor using the first 5 modes

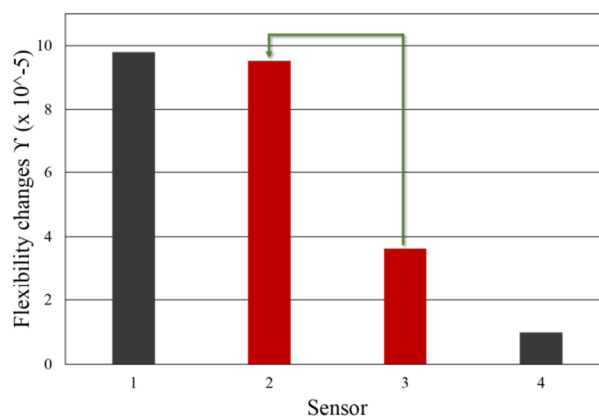


Fig. 8 - Flexibility changes

## CONCLUSIONS

In this paper, a three levels algorithm for Health Monitoring of a 6-storey building FEM was proposed. Starting from output accelerations, it was possible to detect and locate the damage. In the first level, the identification of the Eigen frequencies was carried out using the SSI-COV algorithm under white noise excitation, which helps identify the first 5 Eigen frequencies with accuracy. In the second level, the Eigen frequencies method and the modal assurance criterion were applied to detect the damage. From simulation's results, it was concluded the Eigen frequencies method is a very sensitive damage detector and is easy to set-up. Secondly, the modal assurance criterion allowed the identification of variation of mode shape. In the case of the considered FEM, the variation identified was very small. In order to highlight the mode shape changes it's necessary to increase the number of modes, which is not easily done experimentally. Finally, in the third level, Mode shape curvatures, the curvature damage factor, and the flexibility method have made it possible to detect and to localize damage.

## REFERENCES

- [1]-Abozeid HM, Fayed MN, Mourad SM, et al. Damage detection of cable-stayed bridges using curvature changes in modal mode shapes. International Conference on Bridge Management
- [2]-Systems Monitoring Assessment and Rehabilitation, Cairo, Egypt, 2006.
- [3]-Dawari VB, Vesmawala GR. Structural damage identification using modal curvature differences. IOSR Journal of Mechanical and Civil Engineering, 2013, Vol.4, p. 33-38.
- [4]-Döhler M, Mevel L. Efficient multi-order uncertainty computation for stochastic subspace identification. Mechanical Systems and Signal Processing, 2013, Vol.38, no 2, p. 346-366.
- [5]-Foti D. Dynamic identification techniques to numerically detect the structural damage. The Open Construction and Building Technology Journal, 2013, Vol.7, no 1, p. 43-50.
- [6]-Goursat M, Hermans L, Mevel L. Output-only subspace-based structural identification: from theory to industrial testing practice. Journal of Dynamic Systems Measurement and Control, 2001, Vol.123, p.668-676.
- [7]-Kim JT, Ryu YS, Cho HM, Stubbs N. Damage identification in beam-type structures: frequency-based method vs mode-shape-based method. Engineering Structures, 2003, Vol.25, p. 57-67.

- [8]-Lee YS, Chung MJ. A study on crack detection using eigenfrequency test data. *Computers & structures*, 2000, Vol.77, no 3, p. 327-342.
- [9]-Mevel L, Goursat M. A complete Scilab toolbox for output-only identification. *Proceedings of International Modal Analysis Conference*, Dearborn, Mi. 2004.
- [10]-Ndambi JM, Vantomme J, Harri K. Damage assessment in reinforced concrete beams using eigenfrequencies and mode shape derivatives. *Engineering Structures*, 2002, Vol.24, p. 501-515.
- [11]-Pandey AK, Biswas M, Samman M. Damage detection from changes in curvature mode shapes. *Journal of sound and vibration*, 1991, Vol.145, no 2, p. 321-332.
- [12]-Pandey AK, Biswas M. Damage detection in structures using changes in flexibility. *Journal of sound and vibration*, 1994, Vol.169, no 1, p. 3-17.
- [13]-Pastor M, Binda M, Harčarik T. Modal assurance criterion. *Procedia Engineering*, 2012, Vol. 48, p. 543-548.
- [14]-Peeters B, De Roeck G. Reference based stochastic subspace identification in civil engineering. *Inverse Problems in Engineering*, 2000, Vol.8, no 1, p. 47-74.
- [15]-Reynders E, Pintelon R, De Roeck, G. Variance calculation of covariance-driven stochastic subspace identification estimates. In *Proceedings of IMAC XXV*, Orlando, Florida, USA, 2007, p.169.
- [16]-Rucevskis S, Wesolowski M. Identification of damage in a beam structure by using mode shape curvature squares. *Shock and Vibration*, 2010, vol. 17, no 4-5, p. 601-610.
- [17]-Salawu OS. Detection of structural damage through changes in frequency: a review. *Engineering structures*, 1997, Vol.19, no 9, p. 718-723.
- [18]-Tripathy RR, Maity D. Damage assessment of structures from changes in curvature damage factor using artificial neural network. *Indian Journal of Engineering & Material Sciences*, 2004, Vol.11, p. 369-377.
- [19]-Van Overschee P, De Moor B. *Subspace identification for linear systems: theory, implementation, applications*. Kluwer Academic Publishers, 1996, ISBN-13:978-1-4613-8061-0
- [20]-Wahab MA, De Roeck G. Damage detection in bridges using modal curvatures: application to a real damage scenario. *Journal of Sound and vibration*, 1999, Vol.226, no 2, p. 217-235.

[21]-Wu WH, Wang SW, Chen CC, et al. Application of stochastic subspace identification for stay cables with an alternative stabilization diagram and hierarchical sifting process. *Structural Control and Health Monitoring*, 2016, Vol.23, p. 1194-1213.

[22]-Xie Y, Liu P, et Cai GP. Modal parameter identification of flexible spacecraft using the covariance-driven stochastic subspace identification (SSI-COV) method. *Acta Mechanica Sinica*, 2016, Vol.32, no 4, p. 710-719.

[23]-Yan YJ, Cheng L, Wu ZY, Yam LH. Development in vibration-based structural damage detection technique. *Mechanical Systems and Signal Processing*, 2007, Vol.21, p. 2198-2211.  
Zhang G, Tang B, Tang G. An improved stochastic subspace identification for operational modal analysis. *Measurement*, 2012, Vol.45, no 5, p. 1246-1256.